Supporting Information for

Regulate PD-L1's Membrane Orientation Thermodynamics with Hydrophobic Nanoparticles

Xiaoqian Lin[1,2,3], Xubo Lin[1,*]

1. Beijing Advanced Innovation Center for Biomedical Engineering, Key Laboratory of Ministry of Education for Biomechanics and Mechanobiology, School of Engineering Medicine & School of Biological Science and Medical Engineering, Beihang University, Beijing 100191, China.
2. Shen Yuan Honors College, Beihang University, Beijing 100191, China.
3. State Key Laboratory of Microbial Metabolism, Joint International Research Laboratory of Metabolic Developmental Sciences, Department of Bioinformatics and Biostatistics, National Experimental Teaching Center for Life Sciences and Biotechnology, School of Life Sciences and Biotechnology, Shanghai Jiao Tong University, 800 Dongchuan Road, Shanghai, 200240, China.

*Correspondence to linxbseu@buaa.edu.cn (XL)

1. Methods

Two-dimensional Number Density Map. To investigate whether nanoparticle affects stability of PD-L1 by impacting the overall fluctuation of the membrane, we generated a two-dimensional number density map of DPPC/DIPC/CHOL molecules by using the GROMACS tool *gmx densmap*. All DPPC/DIPC/CHOL COM positions in the last 1 μs trajectory can be mapped to the x–z plane of the lipid membrane. The number density was calculated based on these points on the 2D plane, and all points were colored according to their number density for visualization.

Diffusion Coefficients. The characterize the dynamics properties of the lipids, the lateral diffusion coefficients were calculated from the mean square displacement (MSD) of the molecules in the membrane plane using the GROMACS *gmx msd* tool. The $MSD = \langle |r(t+t_0) - r(t_0)|^2 \rangle$ where r corresponds to the position of the molecular center-of-mass, angular brackets denote time and ensemble averaging. The lateral diffusion coefficient (D) was calculated as a linear-fitted slope using Einstein relation $y = 4D_t + c$. The linear part of the MSD curves, (the MSD-t plot, without the first and last 10%) was fitted to the determine D_t.

Voronoi Tessellation Analysis. The Voronoi tessellation analysis were performed in MATLAB. First, x/y components of DPPC/DUPC center-of-mass coordinates and x/y box dimensions are obtained. Then, the boundary problem was solved by introducing its nearby 8 periodic copies. Last, MATLAB tools such as "voronoin", "polyarea" and "patch" was used to obtained the Voronoi diagram shown in the manuscript (Detailed commands are shown as follows).

```
%Voronoi Tessellation Analysis
A=20;% Input the size of the box.
x=[];% Input x coordinates of per lipid COM.
```

```
y=[];% Input y coordinates of per lipid COM.
x1=x-A;% Periodic boundary.
x2=x+A;
y1=y-A;
y2=y+A;
x0=[x1 x x2 x1 x x2 x1 x x2];
y0=[y1 y1 y1 y y y y2 y2 y2];
[v,c]=voronoin([x0;y0]');
n=length(c);
B=zeros(n,1);
for i = 1:length(c)
C=polyarea(v(c{i},1),v(c{i},2));% Calculate the area value of per lipid.
B(i)=C;
patch(v(c{i},1),v(c{i},2),B(i));% Color according to area value.
set(0, 'defaultfigurecolor','w');
axis([0 A 0 A]),axis square;
```

Contact Number. To investigate the role of surface hydration in PD-L1 in the presence of NPs, the contact number between water and the PD-L1's extracellular domain was calculated for each system using GROMACS tool *gmx mindist* with a cutoff of 0.6 nm.

2. Embedded NPs Affect the Structural Properties of the Lipid Membrane.

We found that the embedded NPs leaded local membrane bending (**Fig. S1**) and the analysis of diffusion coefficient for lipids showed that DPPC/CHOL diffusion coefficient decreased as the number of NPs increased from 1 to 4, but both are higher than that in the NP-free system (**Table. S1** and **Fig. S2**). Besides, the chain order parameters became much more disordered in the system of embedded NPs, the area per lipid and membrane thickness of the system which contained NPs were significantly increased (**Fig. S2**).

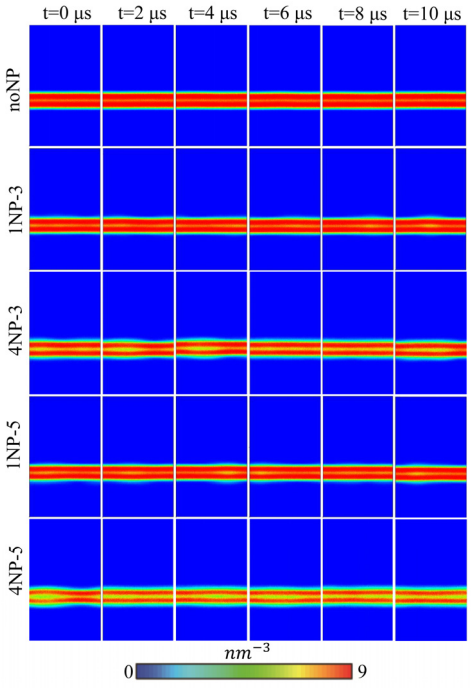

Figure S1. Side-sectional 2D number density map of DPPC/DIPC/CHOL molecules in different systems.

Table S1. The diffusion coefficients of saturated lipids (DPPC), unsaturated lipids (DIPC) and cholesterol (CHOL).

	DPPC $(10^{-5}\,cm^2/s)$	DIPC $(10^{-5}\,cm^2/s)$	CHOL $(10^{-5}\,cm^2/s)$
noNP	0.038 (±0.001)	0.028 (±0.001)	0.057 (±0.005)
1NP-3	0.054 (±0.002)	0.076 (±0.002)	0.079 (±0.002)
4NP-3	0.041 (±0.002)	0.018 (±0.006)	0.070 (±0.004)
1NP-5	0.051(±0.002)	0.063(±0.002)	0.079 (±0.004)
4NP-5	0.042 (±0.002)	0.015 (±0.001)	0.050 (±0.003)

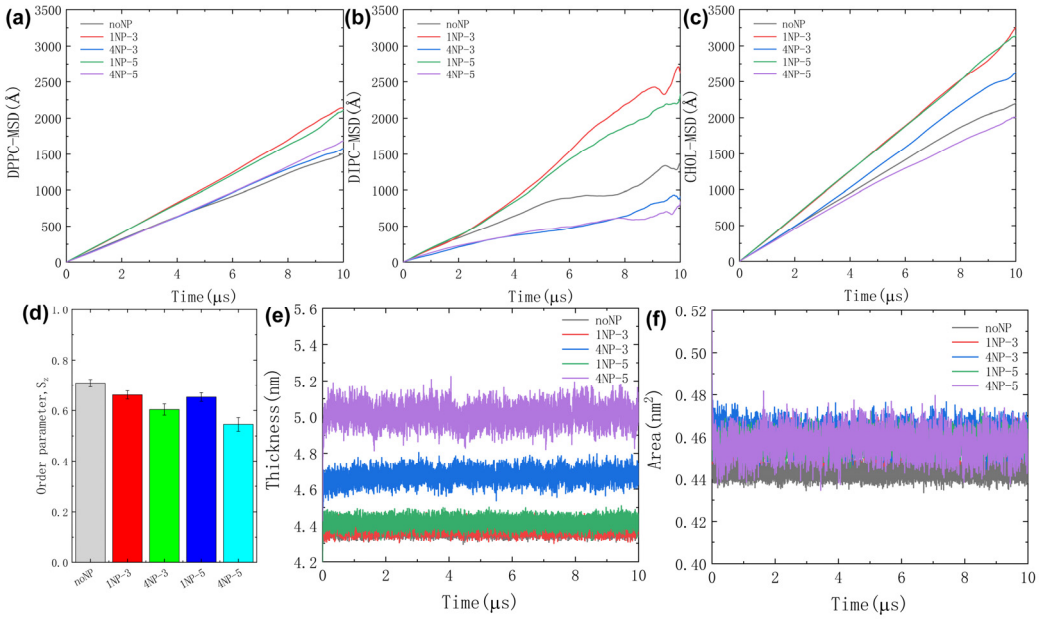

Figure S2. Time evolution of mean square displacement of **(a)** saturated lipids, **(b)** unsaturated lipids and **(c)** cholesterol for different NP-embedded lipid membrane systems. **(d)** Lipid chain order parameter for different NP-embedded lipid membrane systems. Time evolution of **(e)** membrane thickness and **(f)** area per lipid for different NP-embedded lipid membrane systems.

3. NP Concentration and Its Ligand Length Both Affect PD-L1's Membrane Orientation Thermodynamics.

To analyze whether the membrane orientation of the PD-L1 converges during the 10 μs molecular dynamics, we calculated the 2D free energy maps for membrane orientation thermodynamics of PD-L1's extracellular domain of 0-2 μs, 0-4 μs, 0-6 μs, 0-8 μs, and 0-10 μs, respectively (**Fig. S3**). The results showed that the PD-L1's membrane orientation of all systems converged and stabilized as early as 6 μs. The system configuration for typical states of PD-L1 were shown in **Fig. S4**. Furthermore, the corresponding time-varying data for the 2D Gibbs free energy maps shown in **Fig. S5**, which include the time evolution of the membrane orientation thermodynamics of PD-L1's extracellular domain across different systems, as well as the evolution of the distance between PD-L1's extracellular domain and the membrane. To address the size effect of the simulation system, we

conducted additional simulations with larger membrane systems for the case of a single nanoparticle. The simulation box size was increased from 20 nm × 20 nm × 25 nm to 25 nm × 25 nm × 25 nm. The results reveal that in the larger membrane system, the orientation dynamics of PD-L1 remain consistent with our previous findings (**Fig. S6**). This indicates that the membrane size does not significantly affect the nanoparticle-induced modulation of PD-L1's membrane orientation.

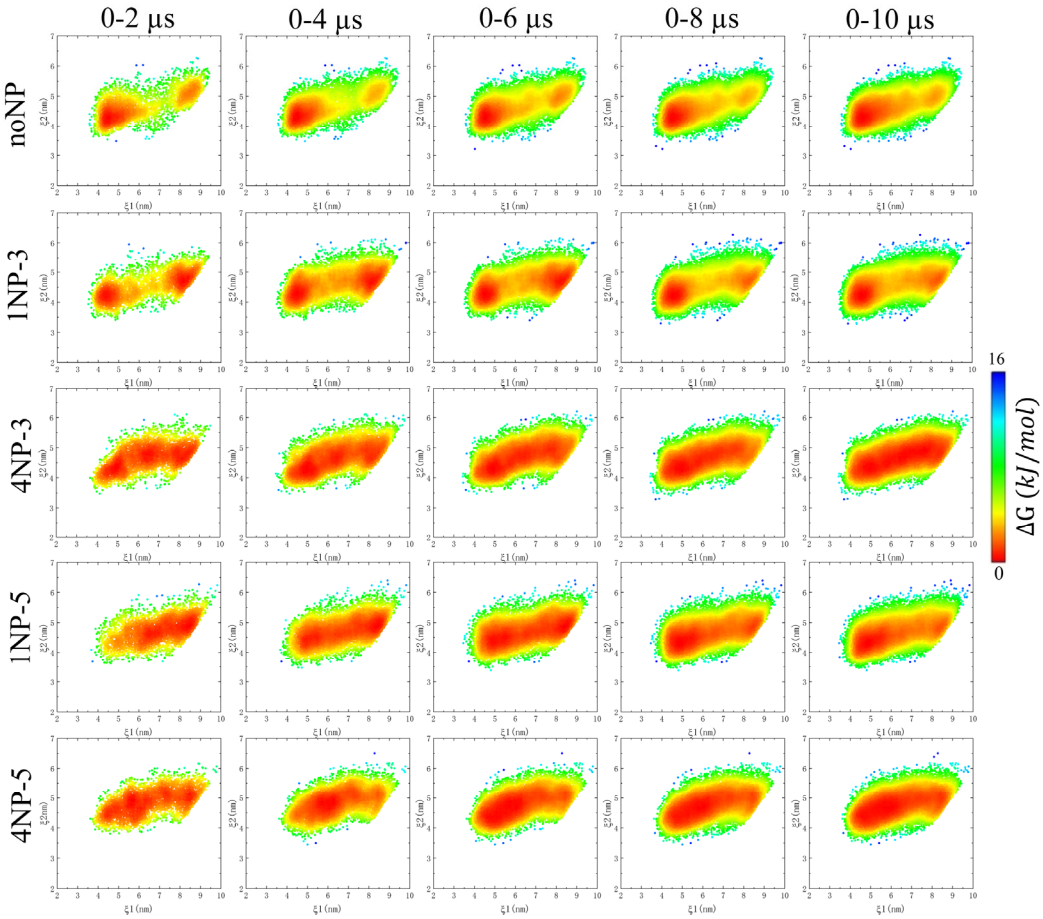

Figure S3. 2D free energy maps for membrane orientation thermodynamics of PD-L1's extracellular domain in different systems.

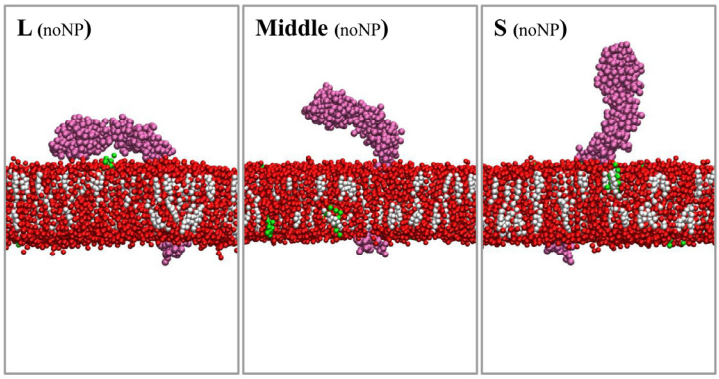

Figure S4. Conformational snapshots for typical states of PD-L1. "S", "L" and "Middle" represents "stand up", "lie down" states and the state between them, respectively.

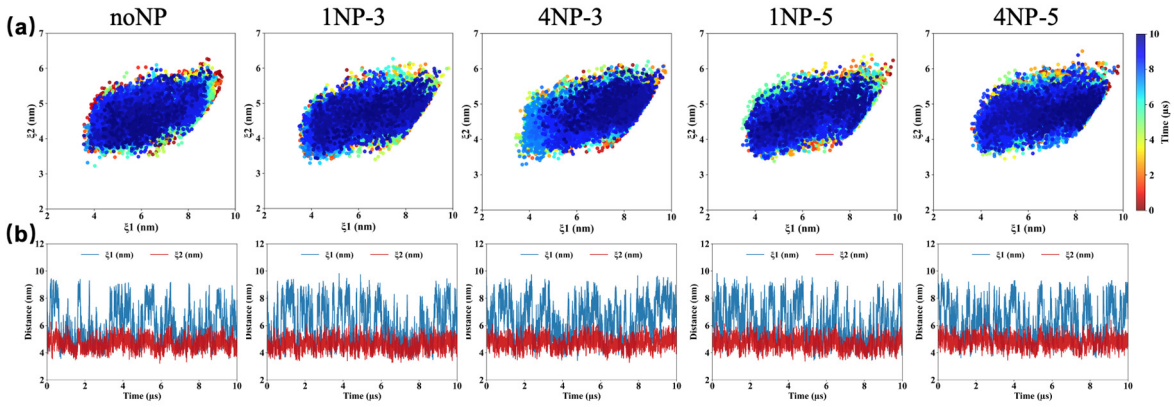

Figure S5. Time evolution of **(a)** the membrane orientation thermodynamics of PD-L1's extracellular domain and **(b)** the distance between the PD-L1's extracellular domain and membrane in different systems. ξ_1 and ξ_2 are center-of-mass distances along the membrane normal (z-axis) between $V1$ (residues 19-127) & $C2$ (residues 133-225) sub-domains of PD-L1 and the lipid membrane respectively.

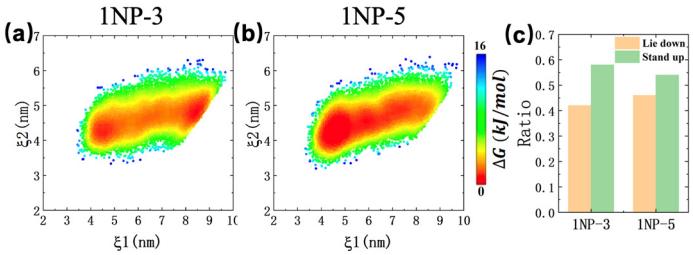

Figure S6. Effects of NPs with different ligand lengths on the orientation thermodynamics of PD-L1's extracellular domain. 2D free energy maps for the membrane orientation thermodynamics of PD-L1's extracellular domain in **(a)** 1NP-3 system and **(b)** 1NP-5 system. **(c)** The ratio of "stand up" and "lie down" in 2D free energy maps. The points with the ξ_1 is distributed less than 6 nm ("lie down") and more than 6 nm ("stand up") points are counted for ratio statistics.

4. Time evolution of contact number of NPs with PD-L1's transmembrane domain.

In our study, NPs may affect the transmembrane domain of PD-L1 by affecting the membrane structural properties around PD-L1. Therefore, the position of NPs within the membrane is particularly important. To investigate this, we analyzed the time evolution of the distance between the NPs and PD-L1's transmembrane domain (**Fig. S7**).

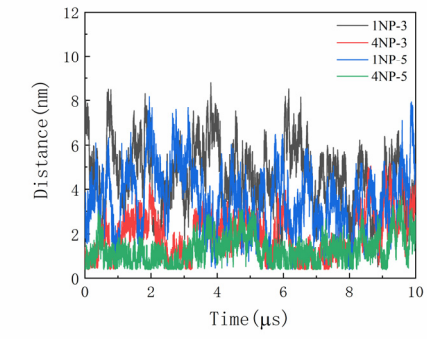

Figure S7. Time evolution of the distance between the NPs and PD-L1's transmembrane domain.

5. Surface hydration of PD-L1 in the presence of NPs.

Protein function is profoundly influenced by both its flexibility and stability in aqueous environments[1-3]. Without sufficient hydration, a protein cannot perform its biological functions. Hydration water plays a crucial role in stabilizing protein structure and facilitating interactions between biomolecules. Protein hydration water refers to the water molecules surrounding the protein within a 0.6 nm shell. This distance corresponds to the end of the second coordination shell of water around a hydrophilic site[4]. To investigate the role of surface hydration in PD-L1 in the presence of hydrophobic ligands and NPs, we calculated the time-varying in the amount of water within a 0.6 nm range of the PD-L1's extracellular domain, along with the distribution probability of water amounts in different systems. The results shows that the decrease in the number of water contacts with PD-L1's extracellular domain in the presence of NPs compared to the NP-free system (**Fig. S8**), which can be attributed to changes in the protein's membrane orientation induced by the NPs. The NP-induced rapid switching of PD-L1's membrane orientation could prevent the formation of a stable hydration layer around the protein. This constant reorientation may disrupt the water molecules bound to the protein, breaking down the structured water shell that typically stabilizes the protein's surface hydration. As a result, the integrity of the hydration shell is compromised, leading to a reduction in hydration.

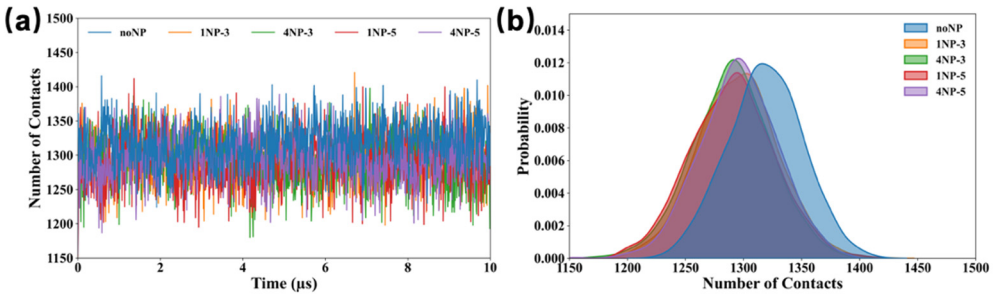

Figure S8. Surface hydration of PD-L1 in the presence of NPs. **(a)** Time evolution of the contact number between the water and PD-L1's extracellular domain. **(b)** Probability distribution of the contact number between the water and PD-L1's extracellular domain in all simulation systems.

References

[1] Grimaldo, M.; Roosen-Runge, F.; Zhang, F.*, et al.*, Dynamics of proteins in solution. *Q. Rev. Biophys.* **2019,** *52*, e7.

[2] Nandi, N.; Bhattacharyya, K.; Bagchi, B., Dielectric relaxation and solvation dynamics of water in complex chemical and biological systems. *Chem. Rev.* **2000,** *100* (6), 2013-2046.

[3] Cametti, C.; Marchetti, S.; Gambi, C.*, et al.*, Dielectric relaxation spectroscopy of lysozyme aqueous solutions: analysis of the δ-dispersion and the contribution of the hydration water. *J. Phys. Chem. B* **2011,** *115* (21), 7144-7153.

[4] Camisasca, G.; Iorio, A.; De Marzio, M.*, et al.*, Structure and slow dynamics of protein hydration water. *J. Mol. Liq.* **2018,** *268*, 903-910.